Effects of cold temperature and main compressor intercooling on recuperator and recompression cycle performance

Weiland, Nathan T.; White, Charles W.; O'Connell, Andrew C.

In: 2nd European sCO2 Conference 2018

2nd European Supercritical CO2 Conference
August 30-31, 2018, Essen, Germany

2018-sCO2.eu-111

EFFECTS OF COLD TEMPERATURE AND MAIN COMPRESSOR INTERCOOLING ON RECUPERATOR AND RECOMPRESSION CYCLE PERFORMANCE

Nathan T. Weiland*
National Energy Technology Laboratory
Pittsburgh, PA, U.S.A.
Email: Nathan.weiland@netl.doe.gov

Charles W. White
KeyLogic
Fairfax, VA, U.S.A.

Andrew C. O'Connell
KeyLogic
Pittsburgh, PA, U.S.A.

ABSTRACT

The performance of supercritical CO_2 (sCO_2) power cycles in general can be improved by reducing the cold sCO_2 temperature in order to increase the sCO_2 density at the inlet to the compressor. This reduces the specific power required for compression and increases the net power and thermal efficiency of the sCO_2 cycle. For similar reasons, the addition of main compressor intercooling typically improves the specific power of a recompression cycle, reducing the sCO_2 mass flow, and thus the required cycle size and cost, for a given power output. The effects of intercooling on cycle efficiency are more complex and require consideration of temperature distributions along the recuperator train.

The present study investigates the effects of cold sCO_2 temperatures, compressor inlet pressures, and number of main compressor intercooling stages, on the efficiency and specific power of recompression Brayton cycles. In particular, it is shown that the addition of main compressor intercooling typically leads to an internal temperature pinch point within the low temperature recuperator. Cycle operation strategies for handling this internal pinch point are discussed, and apply to recompression cycles for all applications, as well as other split-flow cycle types, including partial cooling cycles. Further, internal pinch points and their remediation strategies are also considered for the main CO_2 cooler, as well as for the flue gas heat exchanger, as may be employed in economized recompression cycles for fossil energy applications and cascade-style cycles for waste heat recovery applications. Upfront consideration of these remediation strategies is essential in order to determine attainable cycle operating conditions and component sizing requirements for the sCO_2 cycle.

INTRODUCTION

Much work has been completed in recent years on closed sCO_2 power cycles for a variety of applications, including nuclear, concentrated solar, and fossil-fueled power generation. In most of these studies, the supercritical CO_2 recompression Brayton cycle (sRBC) is employed due to its inherently high efficiency, resulting from both an effective thermal recuperation scheme, and a high average temperature of heat addition at the primary heater. This leads to cycle and plant efficiencies that are typically higher than steam Rankine cycles at comparable operating conditions, as well as the possibility of smaller turbomachinery due to the high overall pressure and low pressure ratio relative to steam cycles.

Figure 1 shows a simplified diagram of the sCO_2 recompression Brayton power cycle. In this diagram, heat enters the cycle from a generic heat source through a primary heat exchanger (PHX) and is delivered to the turbine (T). The partially expanded sCO_2 then cools as it heats the cold high-pressure CO_2 in the high temperature recuperator (HTR) and low temperature recuperator (LTR). On exiting the LTR a portion of the cooled expanded CO_2 is diverted to the recycle compressor (RC) before joining the high-pressure CO_2 exiting the hot end of the LTR and then entering the cold end of the HTR. The non-bypass portion of the cooled CO_2 exiting the hot side of the LTR is then cooled in the primary CO_2 cooler and compressed in the main compressor (MC) before entering the cold end of the LTR. The high-pressure CO_2 is heated in the LTR and HTR before entering the PHX, completing the cycle.

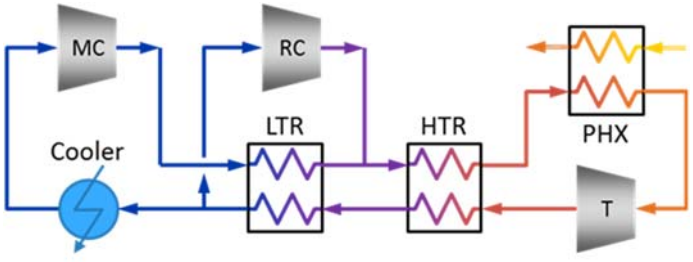

Figure 1: Recompression sCO_2 power cycle

DOI: 10.17185/duepublico/46085

Background

As with any power cycle, the efficiency of the cycle can be increased by either increasing the hot source temperature or decreasing the cold source temperature. A significant feature of these power cycles is their operation in the vicinity of the CO_2 critical point (31 °C, 7.37 MPa) at the cold side of the cycle. For the sRBC, the benefits of reducing the cold sCO_2 temperature are particularly advantageous. Typically, the sRBC efficiency is maximized when the CO_2 entering the main compressor is at or just above its saturation pressure, as shown below. In this regime, lowering the CO_2 temperature increases its density and reduces the specific power required for compression.

Lowering the cooler CO_2 temperature has two additional benefits for the sRBC performance. It allows for an increase in the LTR effectiveness and it makes low temperature heat recovery from process sources or the low temperature region of the heat source a more attractive option. Both of these effects can improve the efficiency of a power plant based on the sRBC: the former by directly increasing the power cycle efficiency and the latter by increasing the quantity of heat harvested by the cycle.

For similar reasons, the addition of main compressor intercooling typically improves the specific power of a recompression cycle, reducing the sCO_2 mass flow, and thus the required cycle size and cost, for a given power output. [1] However, the effects of intercooling on cycle efficiency are more complex and require consideration of temperature distributions along the recuperator train.

Several studies have explored the benefits of reducing the sCO_2 temperature at the cooler. An early study by Wright et al. [2] projected a 4-5 percentage point increase in plant efficiency for a nuclear light water reactor with an sCO_2 power cycle, by moving to condensing cycle operation. An experimental portion of this study proved the feasibility of this concept by demonstrating condensed CO_2 operation of a radial compressor and gas cooler that were designed for gas phase operation near the CO_2 critical point. A later study on sCO_2 power cycles for air-cooled sodium fast reactor nuclear applications shows improvement in cycle performance as the compressor inlet temperature is decreased, as well as variability in performance with compressor inlet pressure. [3]. Similar studies in the nuclear application space have shown that an optimal compressor inlet pressure exists for maximizing efficiency as the compressor inlet temperature is varied. This optimal pressure is typically at [4] or slightly above the pseudo-critical pressure for CO_2 [5].

A recent NETL report examined the cost and performance of a baseline coal-fired oxy-CFB power plant with carbon capture, incorporating the sRBC [1]. The results showed that the CO_2 plant offered a significantly higher efficiency and lower COE than a plant employing a Rankine cycles at operating conditions similar to the sCO_2 plant. The results also showed that a single stage of intercooling for the main compressor offered both higher overall plant efficiency (0.4 – 0.6 percentage points) and a lower cost of electricity (COE, 2.2–3.5 $/MWh) compared to the baseline configuration. More significant improvements in efficiency (0.6 – 1.6 percentage points) are reported in cases where the pressure ratio between intercooled main compressor stages is optimized [6].

Study Objectives

The present study investigates the effects of cold sCO_2 temperatures, compressor inlet pressures, and number of main compressor intercooling stages on the efficiency and specific power of indirect sCO_2 power cycles. In cases where colder sCO_2 temperatures or main compressor intercooling cause temperature pinch point problems in the heat exchangers, options for resolution of these issues are explored, as well as their impact on efficiency and other cycle parameters.

This study is novel in its approach to resolution of internal temperature pinch points in the LTR, which are shown to result from main compressor intercooling. Further, the effect of cold sCO_2 temperature on heat exchanger performance, plant efficiency and specific power is included in this study for both condensing and non-condensing CO_2 cycle operation.

The recompression Brayton cycle is studied in this work, although portions of the analysis apply to partial cooling and cascade cycles as well. Thus the work is relevant to a wide variety of sCO_2 power applications, including nuclear, concentrated solar, fossil, and waste heat sources.

METHODOLOGY

Modeling Approach

The thermodynamic performance of the plant concepts described in this paper are based primarily on the output from a steady-state system model developed using Aspen Plus® (Aspen). The individual unit operations models are the same as those used in the NETL oxy-coal indirect sCO_2 cycle study [1], which included a circulating fluidized bed (CFB) boiler and carbon capture enabled by oxycombustion. Details on the design basis, assumed feed compositions, and state point tables can be found in the NETL oxy-CFB indirect sCO_2 cycle study [1]. This study includes component capital cost estimations, total plant cost calculations, and cost of electricity analyses [1], although these are not considered in this work.

For the boiler and flue gas components of the process, the Aspen Physical Property Method PENG-ROB was used, which is based on the Peng-Robinson equation of state (EOS) with the standard alpha function [7]. This is consistent with the property methods used in other NETL systems studies of power plants with CFB or pulverized coal combustion heat sources.

Accurate modeling of sCO_2 power cycles requires high accuracy in determining the physical properties of CO_2, particularly near its critical point of 31 °C and 7.37 MPa. The Span-Wagner EOS [8] is the most accurate property method available for processes consisting of pure CO_2. Nevertheless, the greatest uncertainty in calculated properties using the Span-Wagner EOS occurs in the region of the critical point [9].

The Span-Wagner EOS is incorporated into the REFPROP (Reference Fluid Thermodynamic and Transport Properties Database) physical property method developed by the National Institute of Standards and Technology (NIST) and is

DOI: 10.17185/duepublico/46085

implemented in Aspen as the Physical Property Method REFPROP [10]. This method was used for all physical property estimates within the sCO_2 power cycle. The power cycle working fluid was assumed to be pure CO_2. Leakage and make-up flows were not modeled.

Modeling of the partial cooling cycle, investigation of solutions to LTR internal pinch points, and other cycle analyses were examined using the REFPROP add-in for Excel [10], which allows for the rapid development of simple cycle models and parametric sensitivity analyses. Analyses using this modeling tool investigate a simple sRBC cycle similar to that of Figure 1, with modifications to include main compressor intercooling and one stage of reheat, but with turbine inlet conditions identical to the more detailed Aspen model. Recuperator temperature profiles are determined in this model by dividing the recuperator into 20 segments of equal heat duty and pressure drop on each side of the recuperator and calculating the resulting sCO_2 temperatures via REFPROP.

Power Cycle: Design, Assumptions, and Operating Point

This study assumes a cycle design that includes a flue gas cooler in parallel with the LTR for the purpose of transferring additional thermal energy from the low quality combustion flue gas to the sCO_2 cycle, as shown in Figure 2. This Figure shows that additional process heat is also recovered from the flue gas in the oxidant preheater and in a nitrogen heater used to regenerate the air separation unit pre-purifier adsorbent. [1] These last integrations aside, this study's analysis of the flue gas cooler is also applicable to the waste heat recovery sCO_2 application, which typically seeks to maximize heat extraction from a low-quality gas turbine exhaust or other combustion flue gas source.

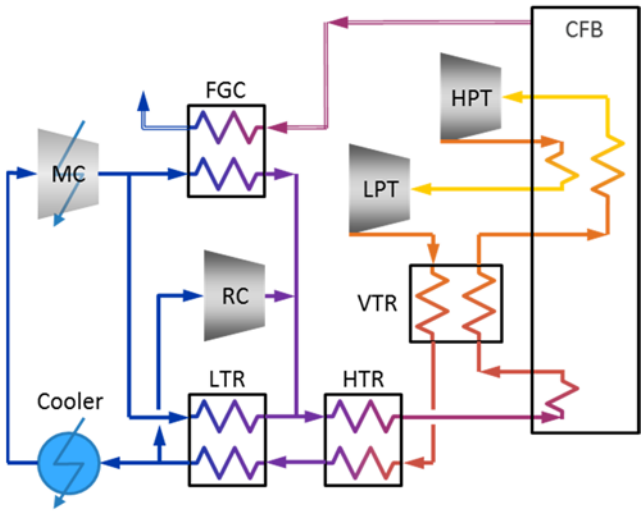

Figure 2: BFD for power cycle used in oxy-CFB power plant

Compared to Figure 1, Figure 2 shows the complete cycle heat integration scheme, a 2-stage turbine with reheat, an intercooled main CO_2 compressor, and a third recuperator stage (VTR) that supplements the HTR by exchanging heat from the relatively high-temperature low pressure turbine (LPT) exhaust with the effluent from an economizer within the CFB. A more detailed process flow diagram depicting all of the major plant components as well as a state point table is provided in Reference [1]. As the present work is primarily focused on process sensitivities around the low temperature components of the cycle, the presence or operation of these other cycle components affects the study results only in that they establish a baseline plant efficiency against which these sensitivities are compared.

In modeling the sCO_2 cycle, the exit temperatures in the recuperators are determined using design specifications within the Aspen model that target a minimum temperature approach at one or both ends of the recuperator of 5.6 °C (10 °F). Similar design specifications are applied to the flue gas and CO_2 coolers.

Second law validation of the heat integration scheme is accomplished from a pinch analysis performed on each heat exchanger in the process. This is done by using multi-stream heat exchanger blocks in Aspen model to represent the heat exchangers and performing granular zone analyses to generate temperature-heat duty (T-Q) and temperature approach-heat duty (ΔT-Q) diagrams for each exchanger.

As a default, the main CO_2 compressor has a single stage of intercooling, although the Aspen model allows a greater number of intercooling stages so that the optimal number of intercooling stages can be determined. In all cases where main compressor intercooling is used, the intercooler outlet temperature is set equal to the main CO_2 cooler outlet temperature, T_{cooler}, and the intercooler pressure drop was set to 0.014 MPa (2 psid). The isentropic efficiencies for each compression stage were equal and the pressure ratios for each compression stage were approximately equal. No attempts were made to optimize the stage pressure ratios in this work, though this may result in additional cycle efficiency gains. [6]

The PHX for the cycle comprises the upper heaters within the CFB in Figure 2, with each heating the high-pressure sCO_2 stream to the turbine inlet temperature of 760 °C. In addition to the economizer in the CFB between the HTR and VTR, a flue gas cooler (FGC) is arranged in parallel to the LTR to recover additional heat from the flue gas, as shown in Figure 2.

Table 1 lists the major assumptions and specifications applied to the sRBC.

Table 1: sCO_2 Brayton cycle parameters

Parameter	Value
Turbine inlet temperature (°C)	760
Compressor outlet pressure (MPa)	34.6
Intercooler pressure drop (MPa)	0.014
Turbine exit pressure (MPa)	7.9
Nominal compressor pressure ratio	3.8
Turbine isentropic efficiency	0.927
Compressor isentropic efficiency	0.85
Cycle pressure drop (MPa)	0.41
Minimum temperature approach (°C)	5.6

In addition to the cycle parameters shown in Table 1, several design variables were adjusted in sensitivity analyses to

DOI: 10.17185/duepublico/46085

thoroughly explore their impact on cycle performance and feasible heat integration. The most important of these was the cooler CO_2 exit temperature, $T_{cooler,}$ investigated for values of 20, 25, 30, 35, and 40°C. Note that the results for a CO_2 cooler exit temperature of 30 °C will be the least accurate due to the limitations of the Span-Wagner EOS near the CO_2 critical temperature of 31 °C. Additional sensitivity design variables were the number of intercooler stages and the intercooler pressure drop, which showed no significant difference in the plant performance when a single stage of intercooling was used.

RESULTS AND DISCUSSION

General Effects of Main Compressor Inlet Conditions

For each cooler CO_2 exit temperature, T_{cooler} examined, a sensitivity analysis was performed on the process (plant) efficiency as a function of the compressor inlet pressure (CIP). The results of these sensitivity analyses are shown in Figure 3.

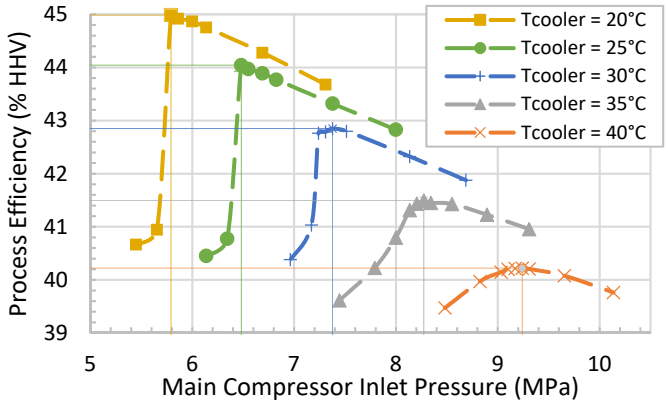

Figure 3: Process efficiency vs. main compressor inlet pressure with one intercooling stage

For each T_{cooler}, a maximum exists in the process efficiency at a particular CIP value. Note that for T_{cooler} below the critical temperature, the plant efficiency is particularly sensitive as the CIP falls below its optimal value. Therefore, in the Aspen model, the actual CIP used was 0.069 MPa greater than the calculated optimal CIP to avoid any convergence difficulties that could occur due to the high sensitivity of the process efficiency at compressor inlet pressures below the optimal value.

Figure 4 shows the points of maximum process efficiency (optimal CIP) as a function of T_{cooler}, as well as the CO_2 saturation line and pseudo-critical line. The optimal CIP for any T_{cooler} is shown to be slightly higher than the saturation pressure or pseudo-critical pressure, consistent with the results of Ref. [5].

A major benefit to reducing T_{cooler}, also the main compressor inlet temperature, is in the significant increase in cycle specific power, defined as the net cycle power output divided by the turbine mass flow. This is depicted in Figure 5 for the sRBC cycle with one main compressor intercooling stage and optimal CIP values per Figure 4. The reduction in T_{cooler} from 40 °C to 20 °C is shown to yield a 35% increase specific power, or viewed another way, a reduction in cycle mass flow by 26% for a fixed cycle power output, which should in turn reduce the capital cost of the sCO_2 power cycle.

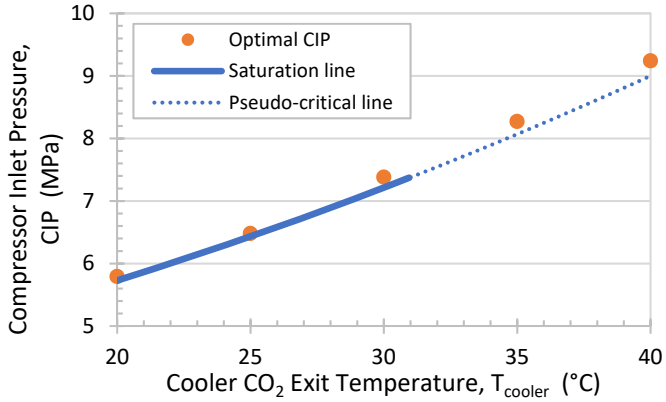

Figure 4: Optimal CIP versus cooler CO_2 exit temperature

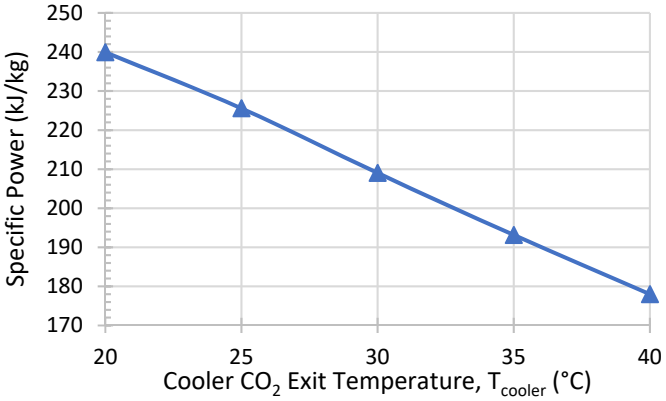

Figure 5: sRBC specific power vs. T_{cooler} for main compressor with one intercooler stage

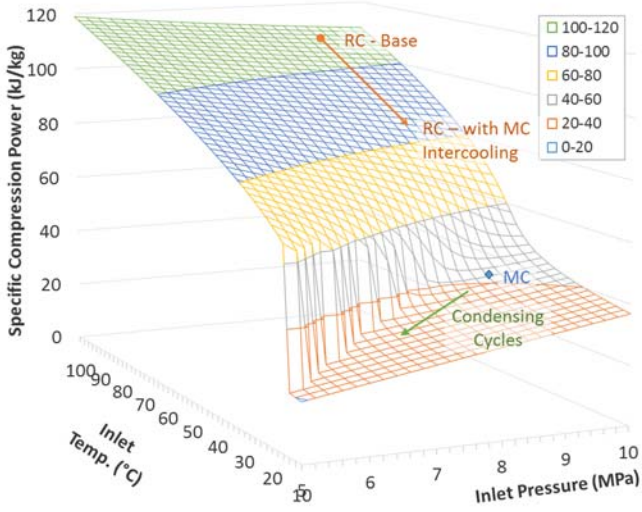

Figure 6: sCO_2 specific compression power for a constant pressure ratio of 4 and η_c = 85%. Compressor inlet conditions are marked for the T_{cooler} = 35 °C case.

DOI: 10.17185/duepublico/46085

The cause of this change is largely a result of reductions in compressor power requirements with increases in sCO_2 density at lower temperatures. This is illustrated in Figure 6, which shows specific compression power (power divided by flow rate) as a function of compressor inlet pressure and temperature. The results are shown for a constant pressure ratio compression process, which gives a sense for the auxiliary load of a recompression cycle with a comparable turbine pressure ratio. Specific compression power is shown to always decrease with compressor inlet temperature. More importantly, it is shown that one of the most significant effects of main compressor intercooling on sRBC performance is to reduce the recycle compressor inlet temperature and specific power consumption (in this case, by about 20%), assuming a constant LTR cold end approach temperature.

Identification of Anomalies in Low Temperature Heat Exchangers

While lowering the cold end CO_2 temperature offers multiple opportunities to increase cycle, and hence, plant efficiency, there are potential disadvantages as well. Low CO_2 temperatures generally require much lower temperature approaches and larger heat transfer areas and costs to attain a desired state point. In addition, low CO_2 temperatures impose limits on the feasible operating point for any given cooling technology. Finally, attaining low CO_2 temperatures on the high-pressure side may require many intercooling stages which may introduce an unacceptable pressure drop in the cycle.

Related to these disadvantages, a sufficiently low CO_2 cooling temperature will create condensation in the CO_2 cooler introducing an internal pinch point into this exchanger. A similar effect can be observed on the hot side of the flue gas cooler if the flue gas temperature falls below the dew point. This latter consideration constrains the maximum amount of heat that can be recovered in the flue gas cooler and diminishes the benefit of intercooling in the main CO_2 compressor.

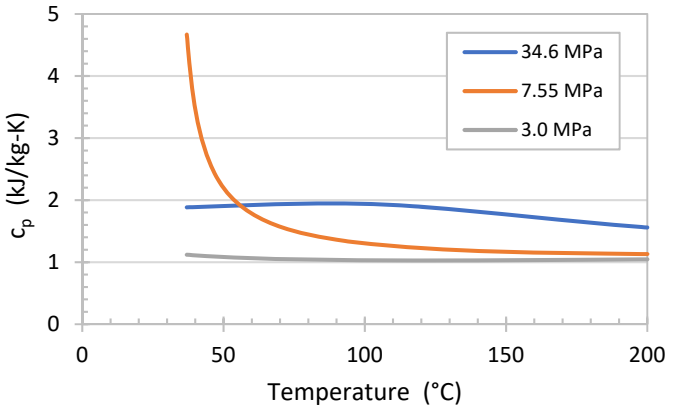

Figure 7: CO_2 constant pressure specific heat (c_p) versus temperature using REFPROP

A final consideration that is unique to sCO_2 power cycles is the rapid and non-linear variation in physical properties, particularly heat capacity (c_p), that occurs in the low temperature end of the cycle. Figure 7 shows the CO_2 c_p over the range of approximately 37 °C to 200 °C, at pressures of 3.0 MPa, 7.5 MPa and 34.6 MPa, typical pressures for the low-pressure side of a partial cooling sCO_2 cycle, low pressure side of a sRBC, and high-pressure side of either a sRBC or partial cooling sCO_2 cycle, respectively.

At the lowest temperatures shown in Figure 7, for the sRBC, the low pressure (hot side) c_p exceeds that for the high pressure (cold side) but this is reversed at temperatures above 56 °C. Further, the high-pressure side c_p has a maximum at a temperature of 88 °C while the low-pressure side shows a near singularity near the CO_2 critical temperature. These phenomena can lead to an internal pinch point and internal minimum temperature approach (below the target specification) in the LTR, even if the minimum temperature approach specification is satisfied at the ends of the LTR.

The use of the recompression configuration is itself an attempt to ameliorate one of the inherent weaknesses of the sCO_2 power cycle, namely that high recuperator effectiveness, which is needed to achieve the highest cycle efficiencies, is hampered by the large thermal capacitance of the cold end high pressure CO_2 compared to the cold end low pressure CO_2 in the cycle.

Note that the nonlinear c_p variation of CO_2 is significantly diminished for the low-pressure side of the partial cooling cycle. Nevertheless, as the temperature increases above 37 °C, the CO_2 c_p for the high-pressure and low-pressure sides diverge, then converge for temperatures above 93 °C. This can also lead to an internal pinch point in the LTR for this cycle, though the problem is generally not as severe as for recompression cycles.

Each of these potential disadvantages were found to impact one or more of the cold end heat exchangers at one or more sets of sensitivity variable values. The following sections describe the impacts to the low temperature flue gas cooler, LTR, and main CO_2 cooler.

Flue Gas Cooler

The flue gas exiting the oxy-CFB has a higher moisture content than would appear in the flue gas for a conventional pulverized coal combustor heat source or an air-fired CFB because a substantial portion of the flue gas is recycled. For the baseline power plant, the recycle fraction was 45% leading to a flue gas moisture content of 20.1% and a dew point temperature of 61.9 °C. Using T_{cooler} = 35 °C and a single main CO_2 compressor intercooler stage, also at 35 °C, the temperature of the CO_2 exiting the main CO_2 compressor is 52.8 °C. Under these conditions, it is infeasible to attain a 5.6 °C minimum temperature approach at the cold end of the low temperature flue gas cooler. Figure 8 shows the T-Q diagram for a flue gas cooler in which the minimum temperature approach specification of 5.6 °C is imposed on both ends of the heat exchanger. The solid lines correspond to the case where a single stage of intercooling is used while the dashed lines correspond to the case where intercooling is not used.

The internal pinch point and temperature cross are clearly evident with a single intercooler. A series of runs on the sensitivity variables showed that condensation occurred in the

DOI: 10.17185/duepublico/46085

low temperature economizer at all T_{cooler} between 20 °C and 40 °C if even a single stage of intercooling is used. If intercooling is not used, condensation in the exchanger did not occur until T_{cooler} fell below 25 °C.

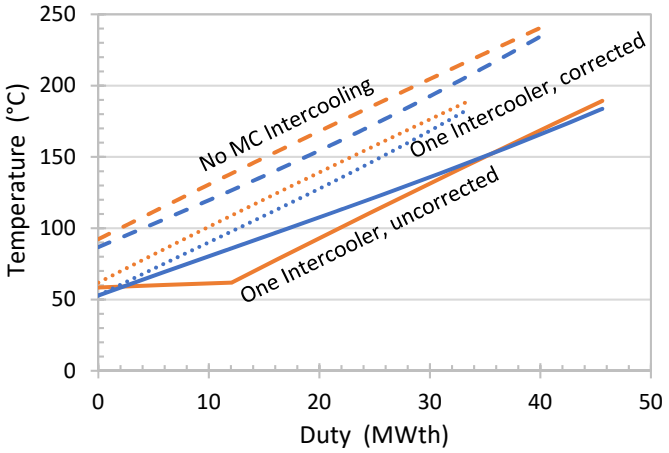

Figure 8: T-Q diagram for flue gas cooler at T_{cooler} = 35 °C. Flue gas on the hot side is in orange, while sCO_2 on the cold side is in blue.

To correct the internal temperature approach arising from condensation within the low temperature recuperator, the hot side (flue gas) exit temperature is limited to its dew point temperature (T_{dew}). This correction is plotted in Figure 8 as well, in which the mass flow rate of the cold sCO_2 is reduced to that required to bring the flue gas to its dew point, reducing the recoverable heat from this heat exchanger.

One alternative to this conservative approach would be to make process changes in the flue gas heat recovery train to remove moisture from the flue gas upstream of the recycle point. This would lower the moisture content of the flue gas and lower T_{dew} which would allow more heat to be recovered from the flue gas. A second alternative approach would allow the flue gas to partially condense up to the point where the minimum approach temperature was achieved.

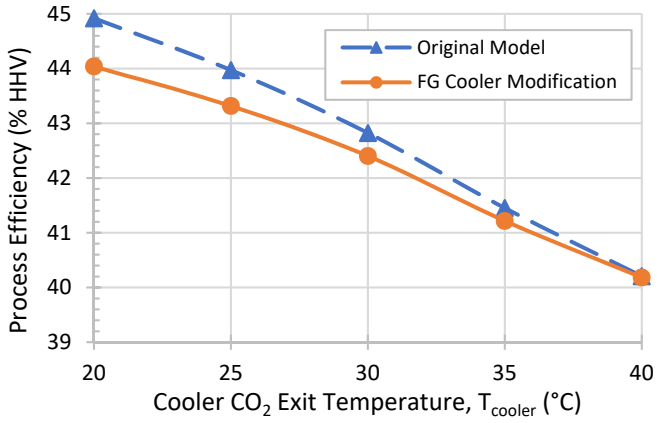

Figure 9: Process efficiency versus T_{cooler}

Figure 9 is a plot of process (plant) efficiency versus T_{cooler} for the baseline plant with one intercooling stage in the main CO_2 compressor. Results are shown for an uncorrected flue gas cooler design in which condensation is occurring and an internal minimum temperature approach exists. Results are also shown for the corrected flue gas cooler design in which the hot side temperature is always maintained at or above T_{dew}.

The results for the corrected flue gas cooler show the same qualitative trend as was observed in the original sensitivity analysis; i.e., the process efficiency increases monotonically with decreasing T_{cooler}. However, the absolute efficiency estimate for the corrected case is approximately 0-2% lower than for the original sensitivity analysis.

Figure 10 shows the sensitivity analysis of process efficiency to the number of intercooler stages in the main CO_2 compressor for T_{cooler} = 35 °C. The results show a similar qualitative behavior to those in Figure 9. The introduction of the design correction lowers the magnitude of the estimated process efficiency by 0-1%, but the qualitative trend in the sensitivity analysis is unaffected. There is a large increase in process efficiency with the introduction of one intercooler stage and a rapid drop-off in the efficiency increase as subsequent intercooler stages are used. Note that there is no impact on the overall efficiency from the flue gas cooler modification when main compressor intercooling is not used.

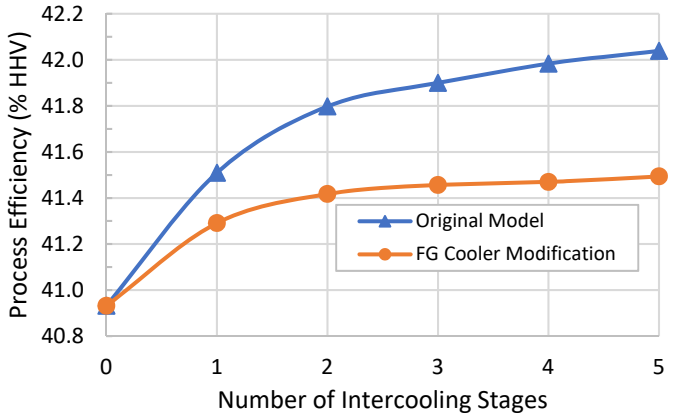

Figure 10: Process efficiency versus number of intercooler stages for T_{cooler} = 35 °C

Figure 11 shows the boiler efficiency (heat transferred to the cycle divided by fuel thermal input to the boiler/heat source) as a function of T_{cooler} when a single stage of main CO_2 compressor intercooling is used. Prior to the design modification to the flue gas cooler, the boiler efficiency increased monotonically with decreasing T_{cooler}, although this was the result of allowing ever larger amounts of water to condense in the flue gas cooler as the CO_2 high-pressure cold end temperature decreased. After the design modification to the flue gas cooler, the flue gas cold end temperature becomes fixed at the dew point temperature so the amount of heat that can be recovered from the flue gas cooler remains constant regardless of the cooler CO_2 exit temperature.

DOI: 10.17185/duepublico/46085

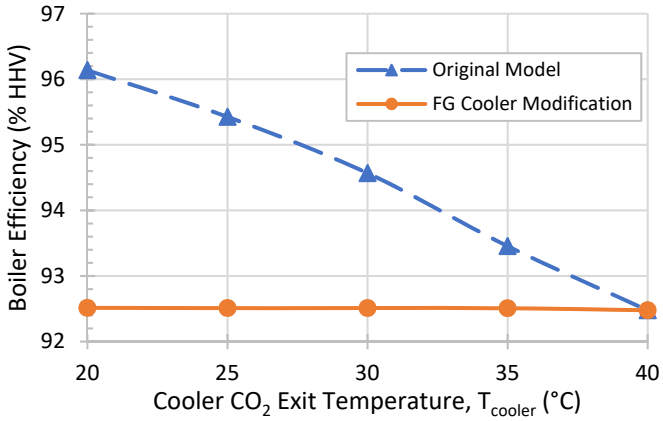

Figure 11: Boiler efficiency vs. T_{cooler}

A similar effect was noted in a sensitivity analysis of the boiler efficiency to the number of intercooling stages. After the flue gas cooler design modification, the cold end temperature was limited to the flue gas dew point temperature whenever intercooling was used, and hence the boiler efficiency remains constant regardless of the number of intercoolers used.

Low Temperature Recuperator

As noted above, the large and non-linear variations in c_p for CO_2 at the low temperature end of the cycle can limit the effectiveness of the LTR. The LTR pinch analysis was conducted for the full range of sensitivity variables and it was found that the addition of main compressor intercooling typically leads to an internal temperature pinch point within the LTR of recompression cycle. Figure 12 shows the LTR temperature profiles for T_{cooler} = 30 °C with a fixed approach temperature of 5.6 °C enforced at either end of the LTR, where the addition of a single stage of main compressor intercooling yields a very close approach temperature near its cold end.

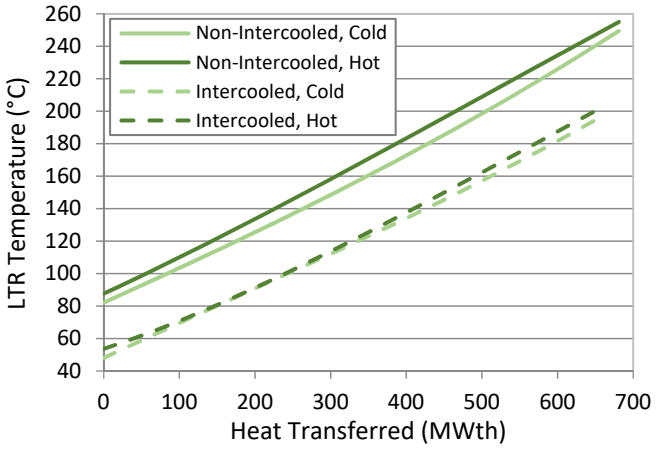

Figure 12: LTR temperature profiles for T_{cooler} = 30 °C as a function of main compressor intercooling

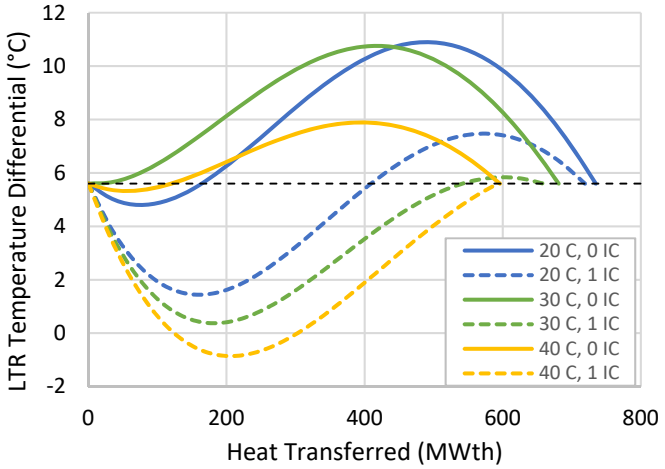

Figure 13: ΔT versus Q for LTR as a function of T_{cooler} and number of main compressor intercooler stages.

This is more readily seen in Figure 13, which plots the temperature difference, ΔT, between the hot and cold sides of the LTR, and also includes data for T_{cooler} values of 20 °C and 40 °C with and without intercooling. For fixed endpoint temperature approaches at 5.6 °C, the addition of intercooling results in very close internal temperature approaches, and even a temperature cross for the 40 °C case, within the LTR, with small internal temperature approaches also occurring without main compressor intercooling in some cases. Similar effects occur, but with a lower temperature differential, for main compressor intercooling in the partial cooling cycle.

Figure 14 shows the ΔT-Q diagram for the LTR for the baseline sRBC plant (T_{cooler} = 30 °C) under various temperature approach specification scenarios. The horizontal dashed line in Figure 14 denotes the target temperature approach of 5.6 °C.

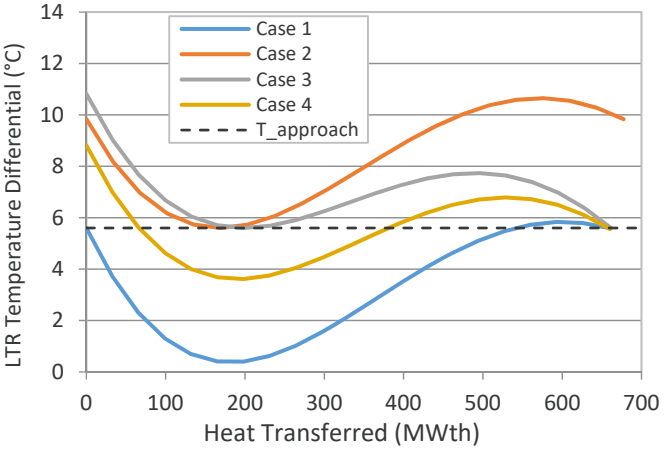

Figure 14: ΔT versus Q for LTR with T_{cooler} = 30 °C

The Case 1 scenario corresponds to the problematic temperature approach specification applied at both the hot and cold ends of the LTR, as shown in Figures 12 and 13, which yields a minimum temperature approach of approximately 0.4 °C

DOI: 10.17185/duepublico/46085

internal to the LTR at the point where approximately 200 MWth of heat has been exchanged. While this scenario leads to the highest cycle efficiency, it clearly violates the intent of the minimum temperature approach specification and is likely infeasible.

For the Case 2 scenario, both the hot end and cold end temperature approaches were increased until the internal temperature approach attained the target minimum of 5.6 °C. This was the most conservative scenario leading to the lowest cycle efficiency.

In the Case 3 scenario, the hot end temperature approach was set to the target value and the cold end temperature approach was adjusted until the internal minimum temperature approach reached the target value. This scenario yielded the maximum cycle efficiency while maintaining the minimum temperature approach specification throughout the exchanger. This is accomplished by increasing the bypass fraction, thereby reducing the cold side sCO_2 flow through the LTR and hence its thermal duty, effectively increasing the hot side exit temperature to increase the cold side ΔT. Note that fixing the LTR's hot end approach temperature, rather than the cold end, decreases the overall temperature difference in the HTR, thus increasing its effectiveness and the overall cycle efficiency. The higher LTR hot end approach temperature for Case 2 is a significant reason for the reduced performance relative to Case 3.

An alternative and less conservative approach is depicted in the Case 4 scenario in which the hot end temperature approach was set to the target value and the cold end temperature approach was adjusted until the average temperature approach throughout the LTR equaled the target value.

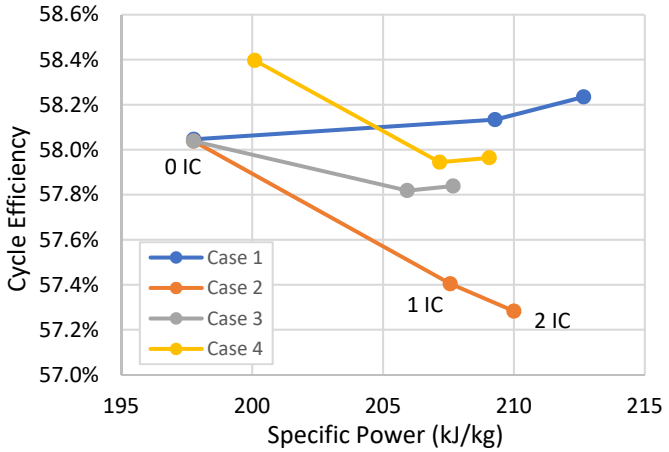

Figure 15: Cycle efficiency and specific power for each Case at T_{cooler} = 30 °C, with number of intercoolers increasing with specific power.

The effects of each LTR temperature approach design strategy on cycle efficiency and specific power is shown in Figure 15. While the Case 1 results show increased efficiency with main compressor intercooling, the internal temperature pinch renders this design infeasible. The remaining strategies generally result in slightly decreased cycle efficiency with main compressor intercooling, though specific power increases in all cases. The preferred strategy is for Case 3, where the minimum LTR temperature approach is strictly adhered to throughout the LTR, while maintaining a higher efficiency than the Case 2 strategy. For Case 3, the size and cost benefits of a 4% increase in specific power are expected to offset the slight reduction in efficiency, thus this design is chosen for most of the remaining analyses, with the expectation that some efficiency may be recovered once the stage pressure ratios are optimized [6].

The same sensitivity analyses as performed for the corrected flue gas cooler case were repeated for the corrected design specification for the LTR. Note that the heat exchanger design corrections were performed sequentially and hence the results for the corrected LTR case also include the correction to flue gas cooler design. Figure 16 shows the sensitivity analysis of process efficiency versus T_{cooler} for the case when one stage of main CO_2 compressor intercooling is used.

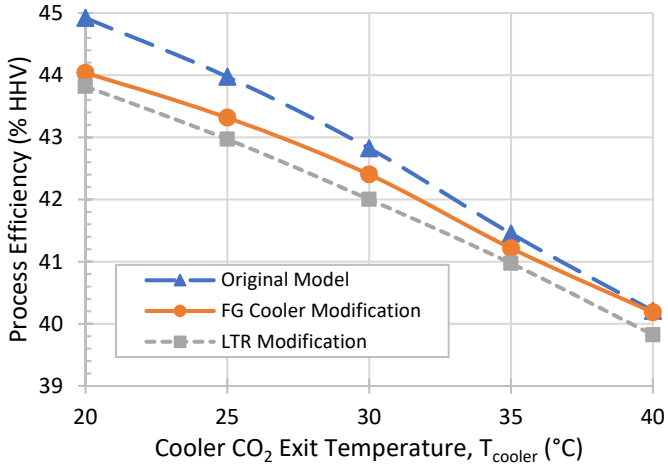

Figure 16: Process efficiency versus T_{cooler}

As with the correction to the low temperature economizer, the correction to the temperature approach specification for the LTR lowered the magnitude of the estimated process efficiency but did not change the qualitative trend of the sensitivity analysis. It appears that the impact of the LTR modification is somewhat less in magnitude than the efficiency change observed after the low temperature economizer modification.

Figure 17 shows the sensitivity analysis of process efficiency versus number of intercoolers at T_{cooler} = 30 °C. The results suggest that applying the design corrections to the low temperature and LTR renders the baseline plant process efficiency relatively insensitive to main CO_2 compressor intercooling.

DOI: 10.17185/duepublico/46085

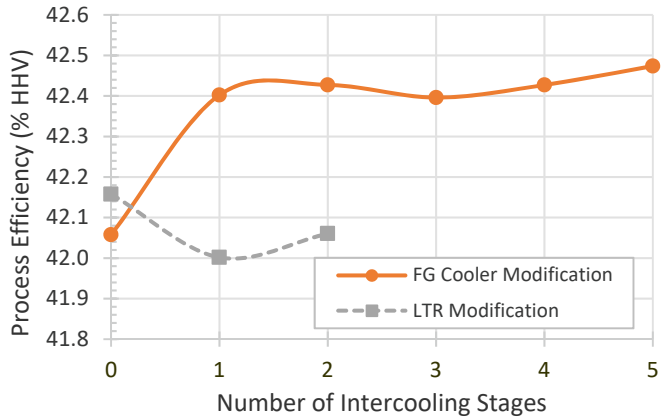

Figure 17: Process efficiency versus number of intercooler stages

Figure 18 shows the specific power as a function of the number of intercooler stages at T_{cooler} = 30 °C. The solid line shows the results after the flue gas cooler design modification and the dashed line shows the results after the flue gas cooler and LTR design modifications. The results show that the LTR modification lowers the absolute value of the specific power when intercooling is used but it does not alter the qualitative dependence of the specific power to the number of intercoolers. As the number of intercooling stages increases, the specific power rises monotonically. However, the most significant increase occurs with just a single stage of intercooling. The increase in specific power with intercooling suggests that intercooling will be economically advantageous as specific power is a surrogate for power cycle size and cost.

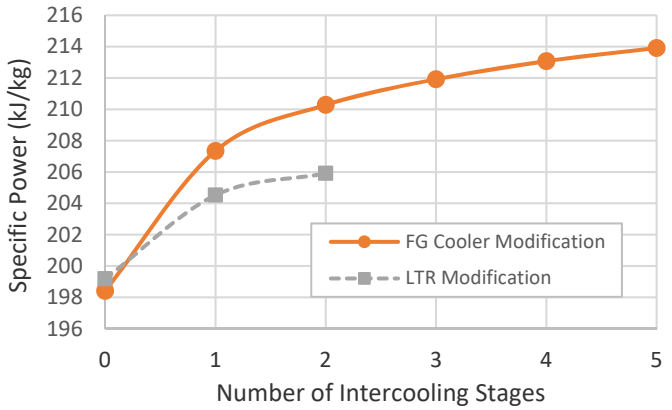

Figure 18: Specific power versus number of intercooler stages

Figure 19 shows the sensitivity analysis for specific power as a function of T_{cooler}. The blue dashed line corresponds to the original heat exchanger configuration, the orange solid line corresponds to the results after the flue gas cooler modification, and the gray dashed line corresponds to the results after the flue gas cooler and LTR design modifications.

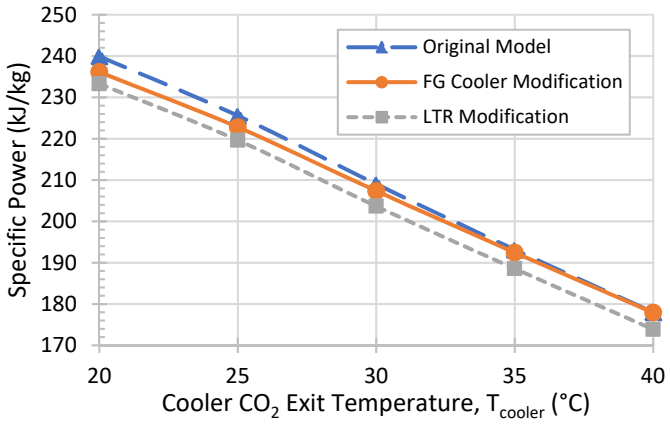

Figure 19: Specific power versus T_{cooler}

The results show that the specific power is strongly dependent on the cooler CO_2 exit temperature and increases monotonically as T_{cooler} decreases. Neither the flue gas cooler modification nor the LTR modification impacted this trend. The net impact of the flue gas cooler modification was to lower the specific power 0-2% while the LTR modification lowers the specific power an additional 1-2%.

Main CO_2 Cooler

This is a straightforward situation in which an internal pinch point can occur in an exchanger when phase change occurs on either the hot or cold side. For the sCO_2 power cycle, this issue is limited to condensing cycles where the cooler CO_2 exit temperature is below the CO_2 critical temperature.

Figure 20 shows the T-Q diagram for the CO_2 cooler in the baseline plant with T_{cooler} values of 25 °C and 20 °C. For both situations, the cooling medium is water with a temperature range from 15.6 °C to 26.7 °C. For T_{cooler} = 25 °C, the CO_2 cooler demonstrates an internal pinch point at the point where the CO_2 begins to condense. The minimum internal temperature approach is 3.7 °C. For T_{cooler} = 20 °C, this shows that the proposed heat exchanger configuration is infeasible due to a temperature crossover.

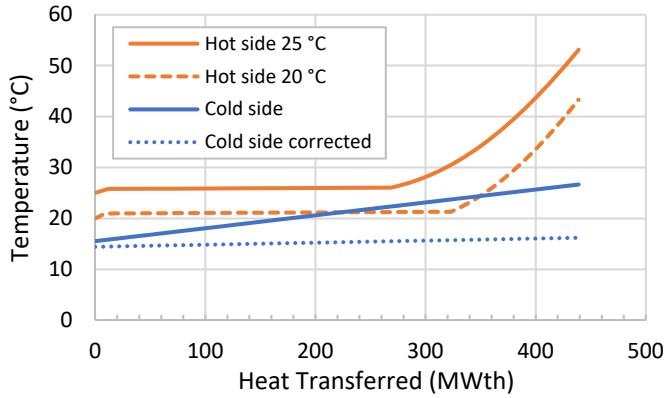

Figure 20: T-Q diagram for the CO_2 cooler, T_{cooler} = 25 °C & 20 °C

DOI: 10.17185/duepublico/46085

A number of strategies exist for addressing an internal minimum temperature approach or potential temperature cross in the CO_2 cooler. One approach would be to reduce the cooling water temperature range by increasing the cooling water flow rate. Another approach would be to reduce the cooling water inlet temperature by altering the cooling tower design. Finally, the target minimum approach temperature in the cooler could be lowered.

The blue dotted line in Figure 20 corresponds to a corrected cooling water configuration that is feasible for the T_{cooler} = 20 °C case. The cooling water inlet temperature was lowered from 15.6 °C to 14.4 °C by lowering the air-water temperature approach in the cooling tower from 4.7 °C to 3.6 °C. This raised the cold end temperature approach to the target value of 5.6 °C. To attain a minimum internal temperature approach or 5.6 °C, the cooling water temperature range was lowered from 11.1 °C to 1.8 °C. While this resulted in a thermodynamically feasible solution, the corrections increased the circulating water flow rate, circulating pump power requirement, and cooling tower fan power requirement by a factor 6. Future work under this study will identify the approach that leads to the lowest COE.

CONCLUSIONS & FUTURE WORK

This study highlights the importance of reducing or minimizing the cold sCO_2 temperature in the recompression Brayton cycle, as a means to increase plant efficiency and specific power, which reduces sCO_2 cycle size and cost. The specific power can also be increased by intercooling the main compressor, though this is shown to cause internal temperature pinch problems in the low temperature recuperator. Several strategies for avoiding these problems are presented, and generally show that maintaining the LTR hot side approach temperature is essential for maintaining cycle performance, while the bypass flow fraction can be increased slightly to reduce or eliminate the internal temperature pinch.

In addition, the effect of flue gas condensation is considered in the flue gas cooler, which can either be in parallel with the LTR in a fossil-fueled recompression cycle, or serve as the primary heat exchanger in a waste heat recovery application. It is shown that main compressor intercooling also increases the likelihood of water condensing out of the flue gas in this heat exchanger, though this is dependent on the water content of the flue gas.

Finally, temperature pinch issues are considered for the CO_2 cooler for cases in which condensation of CO_2 occurs. Several strategies for addressing this problem are considered, but involve a more detailed consideration of the specific cooling system employed, the flow rates and approach temperatures used, and consideration of the overall size and cost of the cooling system.

Future work in this study will focus on performance and cost modeling for direct dry cooling of the sCO_2, indirect dry cooling via water or another heat exchange fluid, and wet cooling towers. These models will be used with existing cost and performance models for the plant, as well as the remediation strategies discussed in this study for handling internal temperature pinches in low temperature heat exchangers as cold sCO_2 temperatures are reduced, in order to optimize the plant's cost of electricity through optimization of the capacity and operation of each type of cooling system.

NOMENCLATURE

ASPEN	-	Aspen Plus
ASU	-	Air separation unit
CFB	-	Circulating fluidized bed
CIP	-	Compressor inlet pressure
CO_2	-	Carbon dioxide
COE	-	Cost of electricity
Compr	-	Compressor
corr	-	Corrected
c_p	-	Heat capacity
CPU	-	CO_2 purification unit
DOE	-	Department of Energy
EOS	-	Equation of state
FG	-	Flue gas
FGC	-	Flue gas cooler
HHV	-	Higher heating value
HPT	-	High pressure turbine
HTR	-	High temperature recuperator
IC	-	Intercooler
LPT	-	Low pressure turbine
LTR	-	Low temperature recuperator
MC	-	Main compressor
NETL	-	National Energy Technology Laboratory
NIST	-	National Institute of Standards and Technology
PENG-ROB	-	Peng-Robinson physical property method
PHX	-	Primary heat exchanger
Q	-	Heat duty
RC	-	Recompression (bypass) compressor, Recompression cycle
REFPROP	-	Reference Fluid Thermodynamic and Transport Properties Database
sCO_2	-	Supercritical carbon dioxide
sRBC	-	Supercritical CO_2 Recompression Brayton Cycle
T	-	Temperature, Turbine
Tapp	-	Temperature approach
T_{cooler}	-	Cooler CO_2 exit temperature
T_{dew}	-	Dew point temperature
TIT	-	Turbine inlet temperature
T-Q	-	Temperature-heat duty
VTR	-	Very high temperature recuperator
ΔT	-	Temperature difference between hot and cold sides within a heat exchanger
η_c	-	Compressor isentropic efficiency

DOI: 10.17185/duepublico/46085

ACKNOWLEDGEMENTS

The authors wish to thank Richard Dennis (NETL) for his support for this project. This work was completed under DOE NETL Contract Number DE-FE0004001. The authors also wish to thank Wally Shelton, Travis Shultz (NETL), Mark Woods, Eric Lewis (KeyLogic) and Dale Keairns (Deloitte Consulting, LLP) for their technical assistance and input.

REFERENCES

[1] National Energy Technology Laboratory (NETL), "Techno-economic Evaluation of Utility-Scale Power Plants Based on the Indirect sCO2 Brayton Cycle," DOE/NETL- 2017/1836, Pittsburgh, PA, September 2017.

[2] S. A. Wright, R. F. Radel, T. M. Conboy and G. E. Rochau, "Modeling and Experimental Results for Condensing Supercritical CO2 Power Cycles," Sandia National Laboratories, Albuquerque, 2011.

[3] T. M. Conboy, M. D. Carlson and G. E. Rochau, "Dry-Cooled Supercritical CO2 Power for Advanced Nuclear Reactors," *Journal of Engineering for Gas Turbines and Power,* vol. 137, pp. 012901-1, 2015.

[4] J. J. Sienicki, A. Moisseytsev and Q. Lv, "Dry Air Cooling and the sCO2 Brayton Cycle," in *Proceedings of the ASME Turbo Expo 2017*, Charlotte, NC, 2017.

[5] S. R. Pidaparti, P. J. Hruska, A. Moisseytsev, J. J. Sienicki and D. Ranjan, "Technical and Economic Feasibility of Dry Air Cooling for the Supercritical CO2 Brayton Cycle Using Existing Technology," in *The 5th International Symposium - Supercritical CO2 Power Cycles*, San Antonio, Texas, 2016.

[6] Y. Ma, M. Liu, J. Yan and J. Liu, "Thermodynamic study of main compression intercooling effects on supercritical CO2 recompression Brayton cycle," *Energy,* vol. 140, pp. 746-756, 2017.

[7] D.-Y. Peng and D. B. Robinson, "A New Two-Constant Equation-of-state," *Ind. Eng. Chem. Fundam.,* vol. 15, pp. 59-64, 1976.

[8] R. Span and W. Wagner, "A New Equation of State for Carbon Dioxide Covering the Fluid Region from the Triple-Point Temperature to 1100 K at Pressures up to 800 MPa," *J. Phys. Chem. Ref. Data,* vol. 25, no. 6, pp. 1509-1596, 1996.

[9] C. W. White and N. T. Weiland, "Evaluation of Property Methods for Modeling Direct-Supercritical CO2 Power Cycles," *J Eng Gas Turb Power,* pp. 140(1):011701-011701-9. doi:10.1115/1.4037665, GTP-17-1264 2018.

[10] E. W. Lemmon, M. L. Huber and M. O. McLinden, "NIST Standard Reference Database 23: Reference Fluid Thermodynamic and Transport Properties-REFPROP, Version 9.1, National Institute of Standards and Technology," National Institute of Standards and Technology, Gaithersburg, 2013.

[11] Q. Zhao, M. Mecheri, T. Neveux, R. Privat and J.-N. and Jaubert, "Thermodynamic Model Investigation for Supercritical CO2 Brayton Cycle for Coal-fired Power Plant Application," in *5th International Supercritical CO2 Power Cycles Symposium*, San Antonio, Texas, March 29-31, 2016.

DOI: 10.17185/duepublico/46085